Simulation of nanocomposite coating created by electrocodeposition method

A. Vakhrushev, E. Molchanov

***Abstract*—**This paper reviews the recent experimental results from literature on electrocodeposition of nanoparticles in a metallic matrix. The mathematical model for hydrodynamic simulation of electrocodeposition of copper and alumina composite coating on rotating cylinder electrode is presented. The model can describe the hydrodynamics, particles size, current density and concentration of particles. It is found that the unsteady diffusion layer is formed close to the rotating electrode surface and the electro kinetics forces are the driving forces of the process. The good correlations with experimental data are received.

***Keywords*—** nanoparticles, electrocodeposition, coatings, composite materials, diffusion layer, current density.

I. Introduction

The composite materials represent the hetero phase system which is consisted of two or more components, that can be classified as reinforcing elements and as a binder matrix The properties of the composite material are determined by the ratio of the parameters of reinforcing elements and binder matrix, as well as of technology their production. As a result of combining of utility of matrix and reinforcing elements it is formed the new complex properties of the composite, which is not only reflects the original properties of its components, but also includes properties that do not had the isolated components.

The composite coating with improved and unique operational characteristics, such as wear resistance, cracking resistance, anti-friction properties, corrosion resistance, radiation resistance and high adhesion to the substrate can be produced by this technology.

There are many kinds of traditional techniques for formation of surface layers with improved physicochemical properties. The most widely used the surface hardening, surface strengthening, and various methods of chemical and thermal machining, for example the carburizing, nitriding, boriding and etc. In recent time the methods influencing on the workpiece surface by beams of particles (ions, atoms, clusters) or high-energy quantum (ion-plasma surface treatment, laser machining) are used extensively. The methods of gas-phase deposition of composite coatings at atmosphere pressure or at vacuum environment have a significantly development. Also the thermal sprayed coating methods receive a powerful development in connection with practical application of technique of plasma and detonation spraying of powdered materials.

A separate new branch of knowledge is the process of composite electrochemical coatings formation [1]-[3].

Metal matrix composite electrochemical coatings (MMEC) are prepared from the suspensions, representing electrolyte solutions with additives of certain quantity of a superfine powder. The particles are adsorbed onto cathode surface in combination with metal ions during electrocodeposition (ECD) process and the metal matrix composite coating is formed. MMEC consists of galvanic metal (dispersion phase) and particles (dispersed phase).

Initially, all electrolyte inclusions are considered as impurities that degraded the quality of the electroplated metal. Efforts were made to prevent incorporation of undesirable particles by enclosing soluble anodes in a bag to prevent dissolved anode material from being codeposited with the plated metal at the cathode or by periodic filtration of electrolyte. Filters were used to remove from the plating solution unwanted suspended particles which could cause dull, rough, and poorly adherent deposits [4].

The first application of MMEC dates back to the beginning of twenty centuries. The nickel matrix with sand particles composite were utilized as anti-slip coatings on ship stairs [3]. Also in 1928 Fink and Prince [5] investigated the possibility of using ECD process to produce self-lubricating copper-graphite coatings on part of car engines. Despite this the systematical scientific investigation of the ECD process occurred only in the early 1960s, immediately after the electrophoretic deposition method has a industrial application for coating metallic substrates by charged particles [6]. In the electrophoretic deposition process, the suspended charged particles moves toward and deposit onto the substrate surfaces as the result of an applied electric field. The codeposition process was developed with the intent of increasing the versatility of the electrophoretic deposition process by combining it with electroplating.

There are the following steps of the ECD process: i) the particles in suspension obtain a surface charge, ii) the charged particles and metal ions are transported through the liquid by

The work was supported by the Kalashnikov Izhevsk State Technical University (S. task 2014/45-1239)

A. V. Vakhrushev is with Kalashnikov Izhevsk State Technical University, 7 Studencheskaya street, Izhevsk, Russia, 426069 (corresponding author to provide phone: +7-3412-214583; e-mail: vakhrushev-a@yandex.ru).

E. K. Molchanov is with Institute of Mechanics Ural Branch of Russian Academy of Science, 34 T. Baramzinoy street, Izhevsk, Russia, 426067 (e-mail: molchanov_86@mail.ru).

the application of an electric field (electrophoresis), convection and diffusion iii) the particles and metal ions are adsorbed onto the electrode surface, and iv) the particles adhere to the electrode surface through van der Waals forces, chemical bonding, or other forces and, simultaneously, adsorbed metal ions are reduced to metal atoms. Metal matrix are encompassed the adsorbed particles and thus the MMEC is formed.

The ECD process is schematically displayed in Fig. 1, 2.

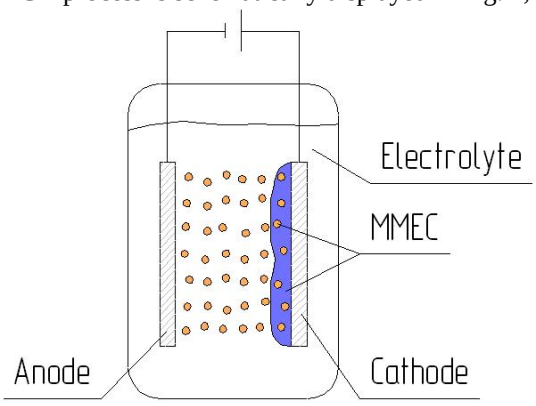

Fig. 1. The ECD process

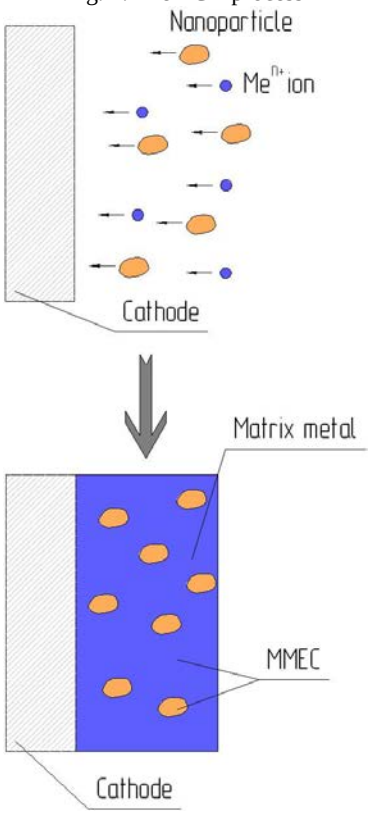

Fig. 2. The process of MMEC formation

The particles of metal including those that can't be electrochemically deposited from water-based electrolytes, synthetic diamond, ceramic or organic materials with dimensions smaller than 100 um are usually used as dispersed phase.

Also the nanomaterials can be employed as the dispersed phase. In accordance with received opinion the nanomaterials are particles with dimensions smaller than 100 nm, also this material is known as ultra dispersed or nanophase material.

Today nanomaterials are may be produced by different methods [7], such as sputtering, laser ablation and condensation in an inert atmosphere, thermal vacuum deposition, pyrolysis, flame hydrolysis deposition, high energy milling, sol gel deposition or electrochemical deposition. Each of these methods has its advantages and disadvantages.

Recent investigations have highlighted that ECD process is an attractive approach for the preparation of nanocomposite coatings.

The advantages of EPD process over other coating methods are the coating uniformity both thickness and chemical composition even for covered detail with complex shapes, reduction of waste often in comparison with dipping or spraying techniques, low levels of environment contamination, the ability to continuously process parts [2]. In addition, ECD process avoids the problems related to high temperature or high pressure processing, also in this method is not necessary to realize the deposition process in vacuum or in an atmosphere of shielding gas.

The low processing temperature (around room temperature) minimizes the inter diffusion or undesirable chemical reactions [3]. The film thickness can be accurately controlled by regulation of the consumed charge.

However, there are a number of problems, such as the nonuniformity of the distribution of nanoparticles in electrolyte volume by reason of agglomeration and sedimentation of particles.

The particles of oxides Al_2O_3 [8], ZrO_2 [9], TiO_2 [10], SiO_2 [11], Cr_2O_3 [12], various allotropic form C [13], carbides SiC [14], WC [15], TiC [16], nitrides Si_3N_4 [17], polymers (polystyrene [18], PTFE [19]) and number of other materials are employed as dispersed phase. Diameter of particles as usual vary from 4 to 800 nanometers. The metals as Cu, Ni, Co, Cr, Zn, Ag, Fe, Au, As or their alloys [20] can be used as dispersion phase.

The concentration of particles suspended in solution are usually varied from 2 up to 200 g/l producing composites with typically 1±10 vol.% of embedded particles [1]-[3]. It has been reported [20] that the incorporation reached up to 50 vol.% when gravity sedimentation was additionally used.

The ECD process is used to produce both soft magnetic materials for sensor implementation [22], and hard-magnetic materials [23]. Moreover, the incorporation of magnetically hard particles of barium ferrites in an electrodeposited Ni or Ni-alloy matrix was found to significantly increase the coercivity of the resulting coatings [24].

The applications of MMEC include wear and abrasion resistant surfaces, lubrication, high hardness tools [25], dispersion-strengthened alloys [26], and for protection against oxidation and hot corrosion [27]. Electrocodeposition process has been used to produce high surface area cathodes which have been used as electro catalysts for hydrogen electrodes in industrial water electrolysis [28].

The process of the ECD finds application in such areas of the industry, as automobile production, building, electric

power production, and also in airspace industry along with oil and gas production.

MMEC based on nickel and aluminum oxides are being applied in different technological fields with high demands on friction and corrosion resistance [8]. The electrocodeposition of SiC nanoparticles into Cu matrix leads to a more appreciable grain refinement and, as a consequence, the nanocomposite coating present a very high micro hardness, 61% higher than pure copper coating, and an increase of 58% of the abrasion resistance [29].

On the electrocodeposition process and hence the structure, the morphology and the properties of the composite coatings is affected next electrodeposition parameters like the electrolysis conditions (composition and agitation of the electrolytic bath, presence of additives, temperature, pH), the electrical profile and the particle properties (type, size, shape, surface charge, concentration and dispersion in the bath), interaction between particles and the electrolyte ions and the character and velocity of fluid motion.

It has been shown [31] that the surface charge of the nanoparticles is an important parameter for the ECD process. An interesting result was that negatively charged particles are more easily codeposited compared to positively charged ones.

The intensity of electrolyte agitation during ECD process is the important factor that affects on the uniformity of nanoparticles distribution in the bulk of electrolyte and on the nanoparticles mass transfer to the electrode surface.

The properties of the MMEC are also strongly influenced by the parameters of the applied voltage. For example, the application of pulsed current [35] deposition provide the deposition of coatings with improved properties such as wear resistance, corrosion resistance surface roughness and grain size in comparison with the direct current deposition. Also, the application of pulsed current in the ECD process allows significantly increase the particles content in the MMEC [1]-[3]. The particles content in the MMEC is a key parameter that determines the properties of the coating such as wear resistance, high temperature corrosion, oxidation resistance, the coefficient of friction. Another important factor is the uniformity of the nanoparticles distribution in the MMEC.

There are a number of types of electrochemical cells which are used in experimental study of the ECD process, such as the parallel plate electrodes, rotating disk [32] or cylindrical electrodes [33],[34], impinging jet electrode (IJE) [35].The IJE provides the selective and high-speed deposition.

The rotating cylinder electrode (RCE) is one of the most common geometries for different types of studies [36], such as metal ion recovery, alloy formation, corrosion, effluent treatment and Hull cell studies. RCEs are also particularly well suited for high mass transport studies in the turbulent flow regime.

In this work the results of mathematical modeling of the ECD process of system Cu-Al_2O_3 on a RCE are presented. The mathematical model describes the mass transfer of electrolyte ions and held in suspension of nanoparticles throughout the volume of the electrolyte, the electrode processes, adsorption and desorption of electroactive ions and nanoparticles on electrode surface and turbulent flow of rotating liquid in electrochemical cell.

In recent years a number of numerical modeling were conducted to study the turbulent flow on RCE. For instance, Perez et al. [36] investigated the copper electrodeposition process on RCE with various applied current density and electrode rotation speed using the standard turbulent model k-epsilon and tertiary current distribution boundary conditions for mass transfer of ions. But in their work the mass transfer of copper ions was investigated only within a tiny stagnant steady diffusion layer. The influence of turbulent flow on the steel corrosion was investigated in [37] where authors were also used the standard turbulent model k-epsilon to modeling the flow. In our work we have found that the Low Reynolds k-epsilon model is more suitable for modeling of the coupled electrochemical processes. The first time ever was found that in the system with the RCE the unsteady diffusion layer is formed and consequently it is necessary to modelling the mass transfer of electroactive ions and nanoparticles thorough the volume of the electrochemical cell.

II. Problem Formulation

The basis for this paper is provided by the fundamental works of Stojak and Talbot [33],[34] where the process of deposition of the Cu-Al_2O_3 MMCC on a RCE was experimentally investigated. In their work the experiments were conducted using a three electrode system, consisting of a RCE, a concentric stationary electrode, and a saturated calomel reference electrode placed in a Luggin capillary. The water solution of 0.1M CuSO4 and 1.2M H_2SO_4 was used as electrolyte. The experiments were conducted at various electrode rotational rates: 500, 1000 and 1500 rpm and concentration of nanoparticles: 39, 120 and 158 g/l. The geometric parameters of electrochemical cell are presented in Fig.3.

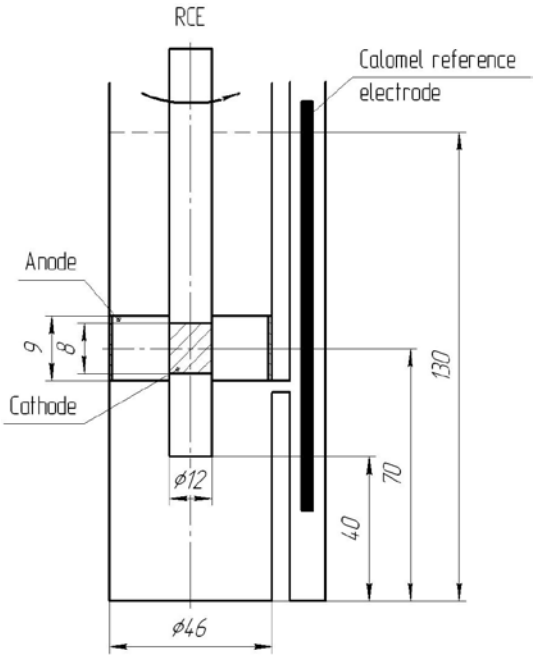

Fig.3. The geometric of cell

The computational domain (Fig.4) is the 2D-axisymmetric space consisting of electrolytic solution, RCE as cathode and anode which is fixed on external cylinder.

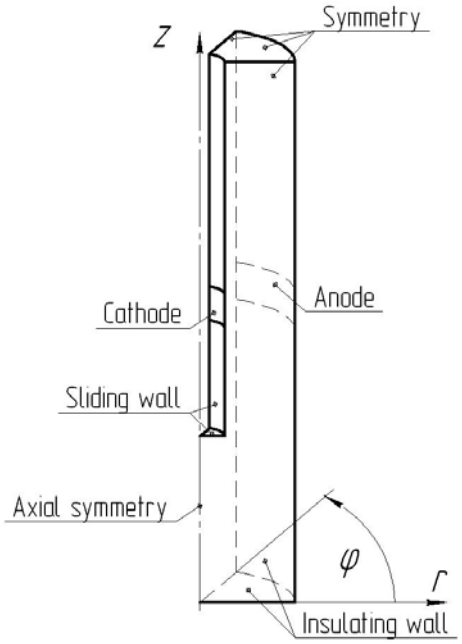

Fig. 4. The computational domain

The hydrodynamics of fluid depends on rotational speed of RCE, electrochemical cell geometric parameters and kinematic viscosity of electrolyte and is possible to characterize by the Reynolds number according to Eq. (1).

$$\mathrm{Re} = \frac{\Omega \cdot r_i \cdot (r_o - r_i)}{\upsilon}, \qquad (1)$$

where Ω is RCE rotating velocity [rad/s], r_i (=6 [mm]) is the radius of the inner cylinder, r_o (=24 [mm]) is the radius of the outer cylinder, υ(=1,155 [mm^2/s]) is the kinematic viscosity. The value of the Reynolds numbers for the deposition conditions of 500, 1000 and 1500 [rpm] are, respectively, equal to 4896, 9792 and 14688. For the system with RCE the critical Reynolds number is equal to 200 [38]. Consequently, the flow of electrolyte has a complex and turbulent nature at all investigated modes and the hydrodynamic of electrolyte turbulent flow is should be accounted in the simulation process.

III. Hydrodynamic Model

Mathematical modeling of the turbulent flow of rotating fluid is still the intractable problem. Application of methods of direct numerical simulation (DNS) and large-eddy simulation (LES) is limited due to the necessity to use a lot of computational power. For this reason the k-epsilon (k-ε) Reynolds Averaged Navier-Stokes (RANS) turbulence model is most commonly used to describe the turbulent motion of the fluid in the numerical modeling of technological processes in engineering calculations [39]. However, this model can be used only to simulate the turbulent flow at some distance from the fixed or moving boundaries and is not suitable for the simulation of rotating fluid [40]. In this model the special wall function is used to describe the flow near the walls since the motion of the fluid near the surface of the border is very different from the motion in the volume. This wall function is represented the analytical expression which depend on flow and grid mesh parameters. For this reason, the computational domain is assumed to be displaced some distance from the wall. The bulk concentrations of electroactive ions at immediate vicinity of electrode surface are necessary to determine in modeling of electrochemical process with account of concentration polarization near the electrode surfaces. Consequently, the k-epsilon RANS model is not suited for modeling of ECD process. In this work we used to describe the turbulent fluid flow the Low Reynolds Number k-epsilon Turbulence Model (low Re k-ε RANS) wherein the wall function isn´t used. There are many different kinds of low Re k-ε RANS model. The most common used models are the Abe-Kondoh-Nagano (k-ε AKN) [41], the Chang-Hsieh-Chen (k-ε CHC) [42], the Launder-Sharma (k-ε LS) [43] and the Yang-Shih (k-ε YS) [44]. The Abe-Kondoh-Nagano (k-ε AKN) model is used in this work as basic model according to the review paper [45], where the above mentioned models were compared.

The system of equations which describe the fluid motion is represented below:

Reynolds Averaged Navier-Stokes (RANS):

$$\rho\frac{\partial \mathbf{U}}{\partial t} + \rho(\mathbf{U}\cdot\nabla)\mathbf{U} = \nabla\left[-P + (\mu+\mu_t)\left(\nabla\mathbf{U} + (\nabla\mathbf{U})^{\mathrm{T}}\right) - \frac{2}{3}\rho\kappa\mathbf{I}\right] + \mathbf{F}, \qquad (2)$$

where **U** is the averaged velocity field, P is the averaged pressure, ρ is the electrolyte density, μ - the dynamic viscosity depends only on the physical properties of the electrolyte, μ_T – the turbulent eddy viscosity (6) which is supposed to emulate the effect of unresolved velocity fluctuations the eddy viscosity, k is the turbulent kinetic energy, ε is the turbulent dissipation rate, F is the volume forces vector.

The continuity equation is:

$$\nabla\mathbf{U} = 0. \qquad (3)$$

The transport equations for turbulent kinetic energy, k, and turbulent dissipation rate,ε, as well as eddy viscosity equation are represented below:

$$\rho\frac{\partial k}{\partial t} + \rho(\mathbf{U}\cdot\nabla)k = \nabla\cdot\left[\left(\mu + \frac{\mu_T}{\sigma_k}\right)\nabla k\right] + P_k - \rho\varepsilon, \qquad (4)$$

$$\rho\frac{\partial \varepsilon}{\partial t} + \rho\mathbf{U}\cdot\varepsilon = \nabla\left[\left(\mu + \frac{\mu_t}{\sigma_\varepsilon}\right)\nabla\varepsilon\right] + C_{\varepsilon 1}\frac{\varepsilon}{\kappa}P_k - f_\varepsilon C_{\varepsilon 2}\rho\frac{\varepsilon^2}{\kappa}, \qquad (5)$$

$$\mu_T = \rho f_\mu C_\mu \frac{k^2}{\varepsilon}. \quad (6)$$

where $C_{\varepsilon 1}$, $C_{\varepsilon 2}$, C_μ, σ_k, σ_ε are the model constant (18), P_k is the production term of turbulent kinetic energy (7) and f_ε, f_μ are the damping functions (8,9).

$$P_k = \frac{\mu_T}{2}\left|\nabla \mathbf{U} + (\nabla \mathbf{U})^T\right|^2, \quad (7)$$

$$f_\varepsilon = \left(1 - e^{-l^*/3.1}\right)^2 \cdot \left(1 - 0.3e^{-(R_t/6.5)^2}\right), \quad (8)$$

$$f_\mu = \left(1 - e^{-l^*/14}\right)^2 \cdot \left(1 + \frac{5}{R_t^{3/4}} e^{-(R_t/200)^2}\right). \quad (9)$$

where l* is the dimensionless number characterizing the distance to the closest wall (10), R_t is the turbulent Reynolds number (11),

$$l^* = \frac{(\rho u_\varepsilon l_w)}{\mu}, \quad (10)$$

$$R_t = \frac{\rho k^2}{\mu \varepsilon}, \quad (11)$$

where u_ε is the Kolmogorov velocity scale(12), l_w is the distance to the closest wall (13).

$$u_\varepsilon = (\mu\varepsilon/\rho)^{1/4}, \quad (12)$$

$$l_w = \frac{1}{G} - \frac{l_{ref}}{2}, \quad (13)$$

where l_{ref} is the characteristic length, which is depended by the model geometry and usually be equal a half of minimal side of rectangle encompassing the model geometry. In this work l_{ref} is taken equal half of radius of external cylinder. The G is the solution of modified Eikonal equation [46].

$$\nabla G \cdot \nabla G + \sigma_w G(\nabla \cdot \nabla G) = (1 + 2\sigma_w) G^4, \quad (14)$$

where σ_w is dimensionless constant range from 0 to 0,5. In this work σ_w is equal 0,1.

The initial condition for equitation is

$$G = \frac{2}{l_{ref}}. \quad (15)$$

The boundary conditions for modified Eikonal equation on insulating and sliding wall boundaries:

$$G = \frac{2}{l_{ref}}. \quad (16)$$

The homogeneous Neumann condition (17) is used on the other boundaries

$$\nabla G \cdot \mathbf{n} = 0. \quad (17)$$

The equation (14) with initial (15) and boundary (16,17) conditions must be solved before starting to solve the main differential equation system.

Following constants are used in this model:

$$C_{\varepsilon 1}=1{,}5;\ C_{\varepsilon 2}=1{,}9;\ C_\mu=0{,}09;\ \sigma_k=1{,}4;\ \sigma_\varepsilon=1{,}5. \quad (18)$$

IV. Electrolyte Substances Mass Transfer

Kinetics of electrode processes depends on the concentrations of ions and particles near the surface of the working electrode, which are known only in the initial moment of the process. They are equal to the concentrations in the bulk solution In well-stirred solution. However, at initial time of deposition process the concentrations of all substances in the electrode-electrolyte surface are changed. Mass transfer layer is formed near the surface of the electrode, the thickness of which depends on the concentration distribution in the bulk solution and the parameters of fluid flow. In a well-stirred solution of electrolyte, the concentrations of active substances is considered to be not change outside of this layer and are equal to they bulk values.

Three mechanisms of mass transfer in the bulk of electrolyte: diffusion, convection and migration, are well known. The mass transfer by diffusion occurs either to the electrode surface or from it, depending on the concentration gradient of the substance. Mass transfer by convection is defined by the terms of hydrodynamic fluid. This process can be created artificially by stirring, but it can also occur in vivo by reason of changes in fluid density. Migration is the third mechanism of mass transfer of substances. It is a result of electrostatic forces, which act only on charged particles and ions in contradistinction from diffusion and convection, which act on the mass transfer of all ions and particles. According to the three mass transfer mechanisms the total substance flow $\mathbf{N}_\Sigma$ is assumed to can be divided into flows of diffusion $\mathbf{N}_d$, migration $\mathbf{N}_m$ and convection $\mathbf{N}_c$

$$\mathbf{N}_\Sigma = \mathbf{N}_d + \mathbf{N}_m + \mathbf{N}_c. \quad (19)$$

The mathematical modeling of mass transfer is performed by means of diffusion-convection equations and is investigated throughout the volume of the electrochemical cell. The electrode processes are described based on the tertiary current distribution boundary condition [47], which is considered the ohmic resistance drop in electrolyte solution, the overpotential on the electrode and ion activity near electrode surface.

The mass transfer equations of electrolyte ions and suspended nanoparticles are defined by the law of conservation of mass:

$$\frac{\partial c_i}{\partial t} + \nabla \cdot \mathbf{N}_i = 0, \quad (20)$$

where subscript i denote Cu^{2+} ions and p denote a nanoparticles. $\mathbf{N}_i$ is the mass flux density of ion or nanoparticle and defined by the Nernst–Planck equation (21).

$$\mathbf{N}_i = -D_i \nabla c_i - z_i m_i F c_i \nabla \varphi_l + c_i \mathbf{u}, \quad (21)$$

where D_i is the diffusion coefficient, c_i is the volume concentration, z_i is the charge number, um_i is the electrophoretic mobility, F is the Faraday constant, φ_l is the electrolyte potential and $\boldsymbol{u}$ is the vector of electrolyte velocity.

The diffusion coefficient of nanoparticles was determinate by using the Einstein's equation (22). The diffusion coefficients of Cu^{2+} ions which were found in the experimental work [34] are used in this work.

$$D_p = \frac{k \cdot T}{6\pi \cdot \mu \cdot r_p}, \quad (22)$$

where k is Boltzmann constant, T is the electrolyte temperature and r_p is the radius of nanoparticles.

Electrophoretic mobility of Cu^{2+} ions and nanoparticles specials are defined by the equitation:

$$m_i = \frac{D_i}{R \cdot T}, \quad (23)$$

where R is the universal gas constant.

The Poisson's equation is used to define the electrolyte potential, φ_l, and to close the system of equations.

$$-\nabla \cdot (\boldsymbol{\varepsilon} \nabla \varphi_l) - F \sum_i z_i c_i = 0, \quad (24)$$

$$\boldsymbol{\varepsilon} = \varepsilon_l \varepsilon_0 \mathbf{I}, \quad (25)$$

where $\boldsymbol{\varepsilon}$ is the permittivity, ε_0 is the permittivity of the vacuum, ε_l is the medium-specific relative permittivity, $\mathbf{I}$ is the unit tensor. The current density depends on the mass flux densities of ions via (26) since ions are both mass and charge carriers.

$$\mathbf{i}_l = F \cdot z_i \cdot \mathbf{N}_i, \quad (26)$$

The electrochemical reaction occurring on electrode surfaces is described by next equation.

$$Cu^{2+} + 2e^- \Leftrightarrow Cu_m^0, \quad (27)$$

where Cu^{2+} denote the Cu^{2+} electrolyte ions, while $Cu_m{}^0$ denote the metal form of copper atoms adsorbed on the cathode and $\Delta\varphi_{eq}$ is the standard electrode potential of reaction (27).

The rates of cathode and anode reactions are defined in accordance with the Butler-Volmer theory [4] by the following equations:

$$i_n = i_0 \left(\frac{c_i}{c_i^b} \right)^{\nu} \cdot \left[\exp\left(\frac{\alpha_a F}{RT} \eta_s^a \right) - \exp\left(\frac{-\alpha_c F}{RT} \eta_s^c \right) \right], \quad (28)$$

where c_i^b is the bulk concentration of Cu^{2+} ions; α_a, α_c are, respectively, the transport coefficients of anodic and cathodic reactions; $\eta_s{}^a$, $\eta_s{}^c$ are, respectively, the over potentials on anode and cathode electrodes.

The over potential is the driving forces for electrochemical reactions, it value can be defined by equation (29).

$$\eta_s^k = V_s^k - \varphi_l^k, \quad (29)$$

where superscript k denote the electrode (a – anode; c– cathode), V_s^k is the potential of respective electrode, $\varphi_l{}^k$ is the potential of electrolyte near the surface of respective electrode.

The cell voltage, U, is the difference between the electric potentials of anode and cathode electrodes.

$$U = V_s^a - V_s^c. \quad (30)$$

The adsorption/desorption processes of nanoparticles on cathode surface are described by (31)

$$P \underset{r_p^d}{\overset{r_p^a}{\Leftrightarrow}} P_a, \quad (31)$$

where P denote the Al_2O_3 nanoparticles suspended in electrolyte volume, while P_a denote the adsorbed nanoparticles Al_2O_3 and $r_p{}^a$, $r_p{}^d$ are, respectively, the rates of adsorption and desorption processes. The assumption that the desorption process is not going on are used in the work The isotherm adsorption (32) is used to describe the process of nanoparticles adsorption

$$r_p^a = k_p^a c_p RT, \quad (32)$$

where $k_p{}^a$ is adsorption coefficient of nanoparticles.

Initial conditions for system of equations are following:

$$c_i = c_{i0},\ c_p = c_{p0}, \quad (33)$$

$$U = f(t),\ \mathbf{u} = 0,\ p = 0, \quad (34)$$

for turbulent kinetic energy, k_0,

$$k_0 = \left(\frac{\mu}{\rho(0.1 \cdot l_{ref})} \right)^2, \quad (35)$$

For turbulent dissipation rate, ε_0,

$$\varepsilon_0 = \frac{C_\mu \cdot k_0^{3/2}}{0.1 \cdot l_{ref}}, \quad (36)$$

Boundary conditions for system of equations are following on electrode surfaces:

$$\mathbf{N}_i = \frac{1}{F \cdot z_i}\mathbf{i}_l, \ \mathbf{N}_\mathrm{p} = r_p^a \cdot \mathbf{n}, \quad (37)$$

on insulating wall:

$$\mathbf{N}_\mathrm{i} = \mathbf{N}_\mathrm{p} = 0, \ \varphi = 0 \quad (38)$$

$$\mathbf{u} \cdot \mathbf{n} = 0, \ k = 0, \ \varepsilon = \frac{2\mu k}{\rho l_\mathrm{w}^2}, \quad (39)$$

on sliding wall:

$$u_r = 0, \ u_\varphi = \omega \cdot r, \quad (40)$$

$$k = 0, \ u_я = 0, \quad (41)$$

$$\varepsilon = \frac{2\mu k}{\rho l_\mathrm{w}^2}, \quad (42)$$

where ω is the RCE rotational speed;
symmetry boundaries:

$$\mathbf{u} \cdot \mathbf{n} = 0, \quad (43)$$

$$\left(-p\mathbf{I} + \mu\left(\nabla\mathbf{u} + (\nabla\mathbf{u})^T\right)\right) \cdot \mathbf{n} = 0, \quad (44)$$

$$\nabla k \cdot \mathbf{n} = 0, \quad (45)$$

$$\nabla\varepsilon \cdot \mathbf{n} = 0. \quad (46)$$

The closed system of equations is received. The model consists of 9 partial differential equation (2, 3, 4, 5, 20, 24). To solve this system of equations a sufficient number of initial and boundary conditions has been given. The finite element method [48] is used in this work to solve this system of differential equations.

V. Results and Discussions

The hydrodynamic modeling of rotating turbulent flow arising in RCE system was done to compare the results of modeling with the well-known experimental data [49]. The standard k-epsilon (k-ε) Reynolds Averaged Navier-Stokes (RANS) turbulence model and Low Reynolds Number k-epsilon Turbulence Model (low Re k-ε RANS) described in this paper were used to determine the more appropriate model. The configuration of system with rotating inner and stationary outlier concentricity cylinders with the geometry parameters r_i=52.5 mm, r_o=59.46 mm, a L=208,8 mm is depicted at Fig.5. The inner cylinder is rotating with the rotating velocity Ω. The modeling was done with a 2D-axisymmetric computational domain during 100s at slowly increasing Reynolds number from 0 to 2000.

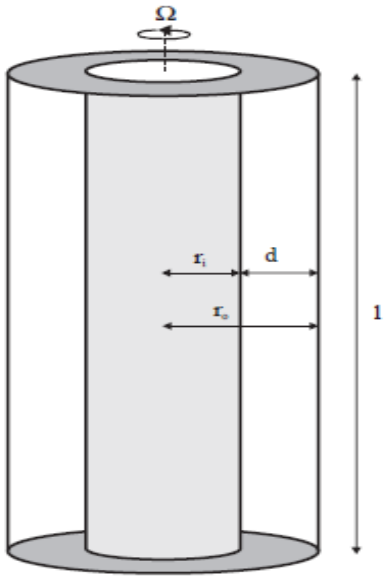

Fig. 5. The geometry of model

In 1923 Taylor [50] found that laminar Couette flow (Fig. 6a) is stable while the Reynolds number of system will not reach the first critical Reynolds number (Re=120), after that the flow is changing to the new form and the toroidal Taylor vortex flow (Fig. 6b) is established. The Taylor vortices are appeared in all volume between cylinders and the order of their disposition relative to the rotation axis is not been changing through time. The Taylor vortices flow is stable in a narrow range of Reynolds number from 120 to 175. The flow is changing to the new form again when the Reynold number of system reaches its second critical value. At this new form the vortices are started to migrate relative to the rotation axis and the wave-vortex flow (Fig. 6c) is established.

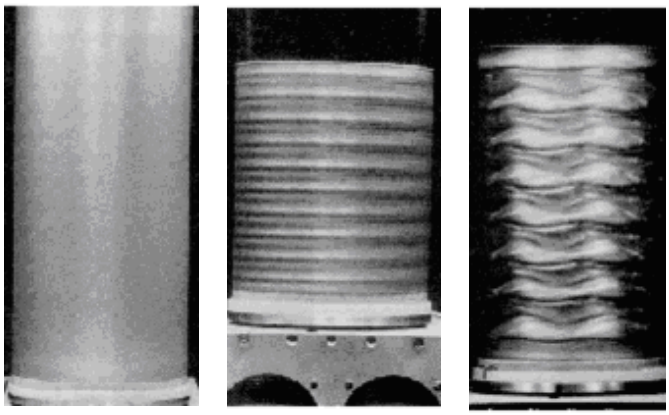

a) Couette flow b) Taylor vortex c) wave-vortex

Fig. 6. The experimental date [49]

The results of mathematical modeling with low Re k-ε RANS model revealed that the laminar Couette flow (Fig.7a) is stable at Reynolds number Re from 0 to 200-250, the Taylor

vortex flow (Fig.7b) is stable at Re from 250 to 1000, after that the wave-vortex flow (Fig.7c) is formed. The wave-vortex flow is stable until the end of simulation.

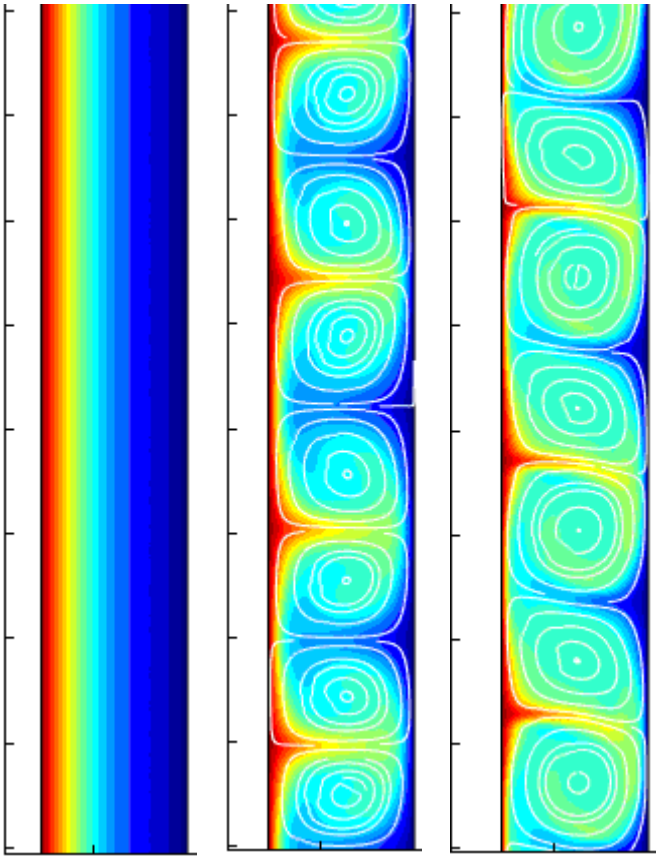

a) Re 200 b) Re 1000 c) Re 1800

Fig. 7. Fields of liquid velocity vector at various Re, m/s

The results of mathematical modeling showed that the standard k-epsilon (k-ε) Reynolds Averaged Navier-Stokes turbulence model isn't appropriated to describe and predict the turbulent rotating flow because the previously mentioned flow changing were not predicted by this model. At this model the quasi-Taylor vortices flow with only one vortex is appeared after laminar Couette flow. The results of modeling with the standard k-epsilon RANS turbulence model are obviously diverging with the experimental date

The mathematical simulation of turbulent flow of electrolyte in RCE cell without considering the mass transfer of electrolyte ion and suspended nanoparticles was also performed in order to examine the flow dynamics at various Reynolds numbers. The rotation speed was gradually increased from 0 to 2000 RPM during 200 s at this simulation. It was found that the flow of the electrolyte at all investigated modes has a complex and turbulent nature. At low Reynolds numbers (Re <400) the flow can be characterized as laminar Couette flow. The flow changing is occurred at Re from 400 to 900, respectively, at 41 and 92 [rpm]. However, at this Re the Taylor vortices are not formed in contradistinction from the case of fluid motion between two concentric cylinders but a lot of small vortices are formed and have been moved chaotic relative to the axis of rotation of RCE.

Hydrodynamic mathematical modeling of the electrodeposition of copper on RCE was conducted at three various rotational speed of the inner electrode 500, 1000 and 1500 rpm in accordance with the experimental conditions [33],[34]. The process of electrocodeposition of Cu-Al_2O_3 nanoparticles was simulated at three various concentrations of nanoparticles 39, 120 and 158 g/l only at 1500 rpm. The computional time was limited by 105 s. At this time the rotational velocity of RCE and cell voltage varies from the open circuit value (+0.037mV vs SCE) to -0.5 V at a scan rate of 5 mV/s according to Fig.8.

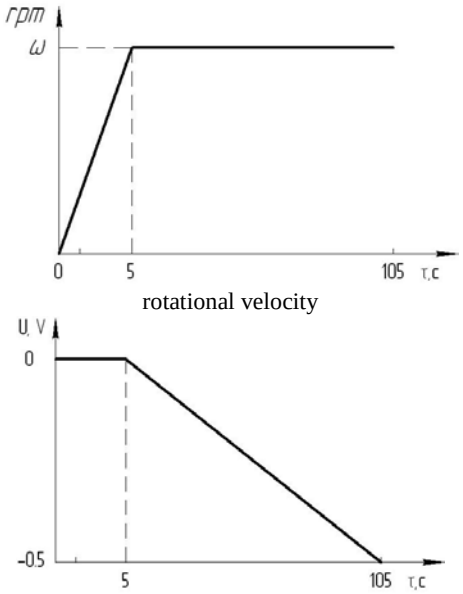

Fig. 8. The modeling parameters

The result of hydrodynamic mathematical modeling of Cu electrodeposition found that the flow has a developed turbulence character at all investigated rotation speed (Fig.9) in accordance with the results which were mentioned above. It also was defined that the zones with high and low fluid velocity are continuously formed near the electrode surface.

The following results apply to all investigated modes: when the voltage between the electrodes reaches the magnitude of -0.4 V relative the calomel reference electrode the concentration of Cu^{2+} ions near the cathode surface is reduced to values close to zero. Consequently, strong concentration polarization is occurring at this cell voltage and the current density is achieving limit value. Therefore, the mass transfer of electro active ions to the electrode surface by diffusion becomes the time-dependent step which determines the rate of electrochemical reaction at the electrode.

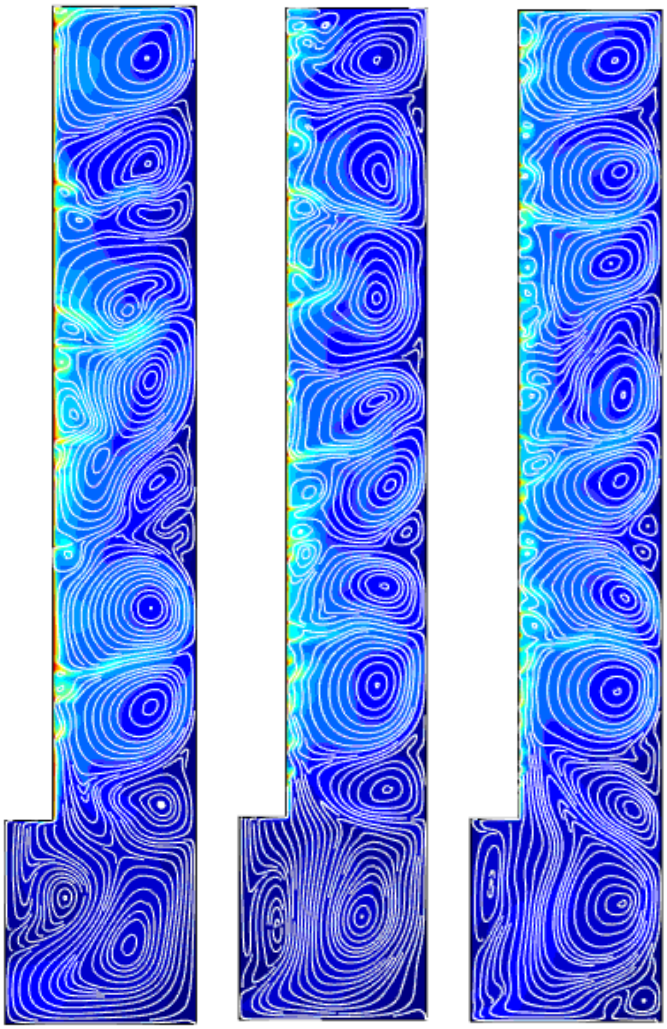

a) 500 rpm b) 1000 rpm c) 1500 rpm

Fig. 9. Developed turbulence in the operating conditions of the electrochemical cell

The rate of ECD process reaches a certain limiting value because rate of diffusion is limited

It should be pointed out that when the diffusion-controlled stage of deposition process has been achieved the oscillation of current density appears at all operating modes of electrochemical cell (Fig.10-12). It is the author's opinion that these oscillations occur by reason of turbulent flow near the electrode surface and because the regions with high or low electrolyte motion speed are continuous appearing near the electrode surface and are being replaced by each other. In consequence of which the stagnant zones with relatively small ion concentration is being arisen from time to time near electrode surface. It means that the diffusion layer, which have a larger thickness, arisen too. In its turn this increases the time, which wanted to transfer the electro active ions to the electrode surface by means of diffusion, and, respectively, decreases the current density. The mass transfer of ions to the cathode surface by convection is increased when a zone with a high velocity of electrolyte reaches the electrode surface. As a result of this the thickness of diffusion layer and, consequently, the time which is required to delivering the Cu^{2+} ions to the cathode surfaces by means of diffusion, are decreasing and the local current density is temporarily increasing. More detailed results of hydrodynamic mathematical modeling of electrocodeposition process presented in the paper of authors [51].

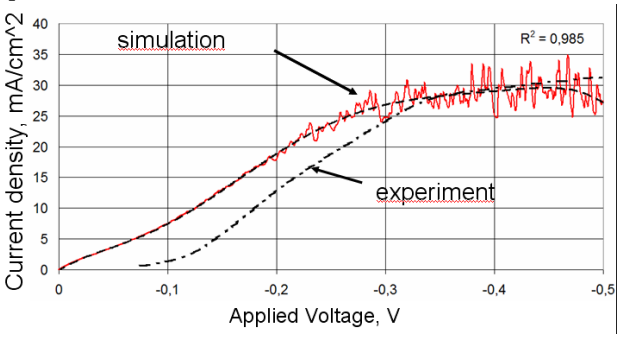

Fig. 10. Current density at 500 rpm of RCE without nanoparticles

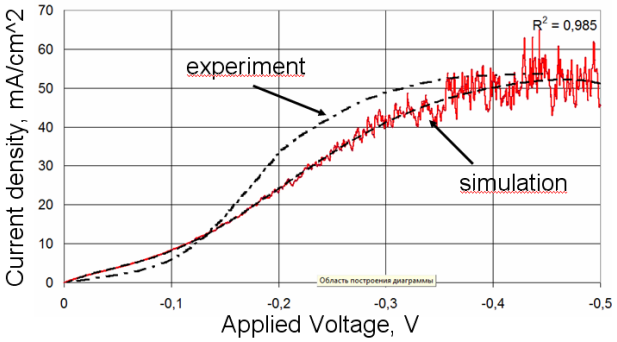

Fig. 11. Current density at 1000 rpm of RCE without nanoparticles

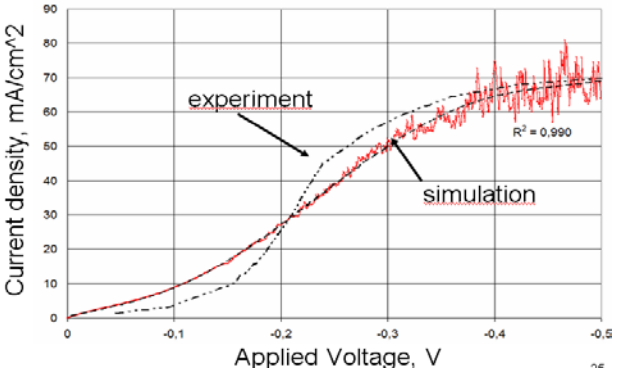

Fig. 12. Current density at 1500 rpm of RCE

The diffusion layer thicknesses are varied in sufficient wide range, so the diffusion layer thicknesses are changed from 30 to 60, from 20 to 50, from 15 to 40 μm for rotational velocity of RCE 500, 1000 and 1500 rpm, respectively.

In 1954 Eisenberg, Tobias and Wilke [52] determined the empirical relationship for limiting diffusion current density which is commonly used in theoretical electrochemistry:

$$i_L = 0.0791 \frac{nFDC}{2r_i} \left(\frac{\nu}{D} \right)^{0.356} \mathrm{Re}^{0.7} \qquad (47)$$

,

here n, D and F are, respectively, the charge number, the diffusion coefficient and the bulk concentration of electroactive ion, F is the Faraday constant. The values of limiting diffusion current density are shown in the table 1 for

the investigated system configurations. Based on the Brunner's correlation the equation of the thickness of the diffusion layer has the form:

$$\delta = 15{,}562 \cdot D^{0.356} \cdot \nu^{0.344} \cdot \Omega^{-0.7} \cdot r_i^{-0.4}, \qquad (48)$$

The analysis of equation (43) shows that the thickness of the diffusion layer is depended only on geometry of the electrochemical cell, kinematic viscosity of the electrolyte, diffusion coefficient of species and electrode rotational velocity and is not depended on the time during which the process is carried.

Table 1 Current density.

Denotation	Limited current density, mA/cm^2 (Error, %)		
RCE rotating velocity rpm	500	1000	1500
Experiment	31	50	67
Calculation, (Eq.42)	39,3 (26,9%)	63,9 (27,8%)	84,9 (6,7%)
Simulation	29 (6,4%)	51,6 (3,2%)	67,1 (0,15%)

Table 2 The diffusion layer thickness.

Denotation	Thickness of diffusion layer, μm		
RCE rotating velocity, rpm	500	1000	1500
Calculation, (Eq.43)	32,369	20,069	14,977
Simulation	30-60	20-50	15-40
Reynolds number	4896	9792	14688

Results of mathematical modeling are proved that the diffusion layer is unsteady. Consequently, the paradigm of steady diffusion layer [52] is not fully sufficed to the RCE when turbulent flow is stated. In order to advance the understanding, the nature of electrochemical process it is necessary to modeling the coupled process which takes into account the hydrodynamic of electrolyte flow.

Usually [4], the influence of electro kinetic forces on mass transfer of electroactive ions are not considered into mathematical modeling of conventional electrochemical processes like a cathodic metal reduction because these processes are carried out in the solution of strong electrolytes with high electric conductivity. However, this assumption is not appropriate when a modeling of ECD process is carried out, since the electro kinetic forces have a significant influence on mass transfer of nanoparticles. Because the double electrical layer (DEL) is formed around nanoparticle suspended in electrolyte solution [4]. The structure of DEL is significantly varied depending on composition and concentration of electrolyte, material, shape and dimension of the nanoparticles.

The DEL structure is usually characterized by the zeta potential, which can be positive, negative or equal zero. During ECD process the nanoparticles with positive zeta potential are additionally attracted to the negatively charged cathode due to electrokinetic forces, while the nanoparticles with negative zeta potential are repelled from it. In its turn the electrokinetic forces doesn't influence on masstransfer of nanoparticles with zero value of zeta-potential.

The analysis of the experimental results [33],[34] revealed that the nanoparticles weight content is slowly reduced with increasing of current density. However, despite this the nanoparticles flow to the cathode surfaces have to increase with increasing of current density. Because according to the Faraday's law the flow of reduced ions increases with increasing of current density. Consequently, the proportional increasing of nanoparticles flow is necessary to keeping the weight content with the increasing of current density. This is confirmed by the Fig.13, which depicted the adducted dependences of nanoparticles flow as function of applied current density and initial concentrations of nanoparticles.

The Fig.13 revealed that the nanoparticles flows are linearly increased with increasing of current density and consequently voltage of electrochemical cell. This means that the influences of electro kinetic forces on mass transfer of nanoparticles must be accounted in the mathematical simulation and that the nanoparticles used in the basic experimental work [33],[34] should have a positive zeta potential, because they flow are linearly increases with increasing of the cell voltage.

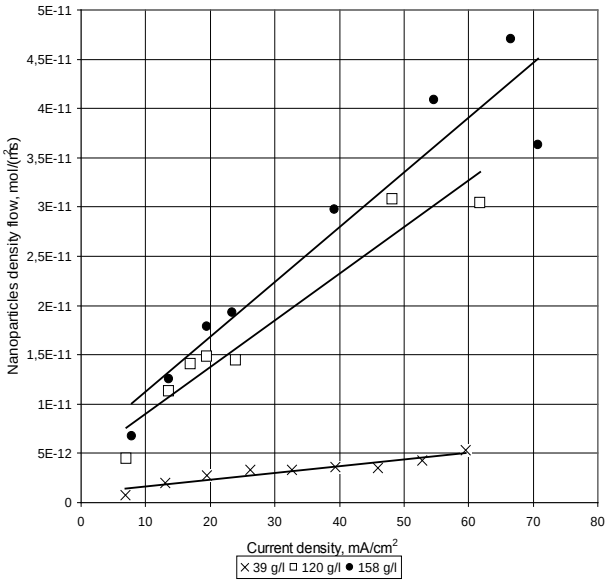

Fig. 13. The adducted dependences of nanoparticles flow

In the work [53] authors revealed that zeta-potential of nanoparticles is the main factor, which determines the nanoparticles weight content in composite coating. They discovered that the α-Al_2O_3 and γ-Al_2O_3 nanoparticles have, respectively, positive and negative zeta-potential in

experimentation conditions. They also found that only α-Al_2O_3 nanoparticles are effective for codeposition with Cu at the same experimental condition.

In the basic experimental work [33],[34] authors point out that they for the first time ever obtained the MMEC of copper with γ-Al_2O_3 nanoparticles. However, based on the data of experimental work [53], the γ-Al_2O_3 nanoparticles should have a negative zeta potential for electrolyte concentration used in the work [33],[34]. The surfactants which could change the sign of the zeta potential of nanoparticles in [33],[34] were not used. Therefore, the electro kinetic forces should prevent the codeposition of γ-Al_2O_3 nanoparticles and the formation of the CEP with the γ-Al_2O_3 nanoparticles could not occur.

However, as established by the authors [33],[34] used nanoparticles γ-Al_2O_3 were a powder mixture of γ-Al_2O_3 nanoparticles with the low presence of α-Al_2O_3 nanoparticles. And thus, the nanoparticles used in [33],[34] were a two-component mixture. The actual ratio between phases has not been determined in the work of the authors. However, according to the authors of this paper the concentration of each phase can be approximately determined from the difference between the densities of the powder mixture of nanoparticles measured in [34] and reference values of density of α- and γ-Al_2O_3 nanoparticles. It was determined the approximate ratio between γ-Al_2O_3 and α-Al_2O_3 phases on the basis of the calculation, which is not given in this article. It was found that the γ-Al_2O_3 nanoparticles comprise 88.3 of weight percent of powder mixture, while the α-Al_2O_3 comprise only 11,7% of weight percent of powder mixture. Based on the foregoing, it is assumed that instead γ-Al_2O_3 with an initial concentration of nanoparticles in electrolyte bath the α-Al_2O_3 nanoparticles are taken into consideration in this work with concentration of 11.7% from initial.

The resulting dependencies of weight content on applied current density are depicted in Fig.14. The good agreement with experimental data [33],[34] has been obtained.

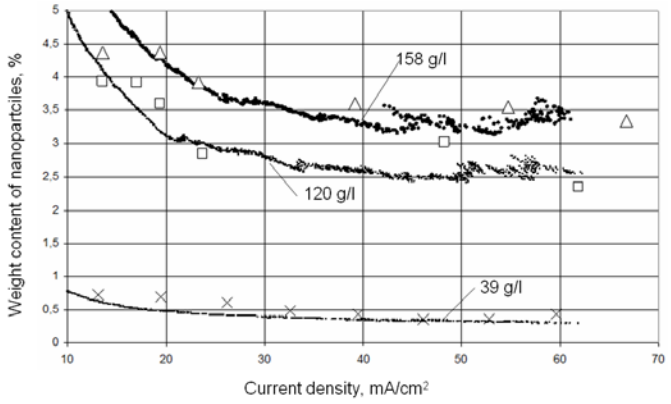

Fig. 14. dependencies of weight content on applied current density

VI. Conclusions

The results of mathematical modeling of copper and alumina particles ECD on RCE with consideration of electrolyte turbulent flow are presented. A good correlation with the published experimental date [33],[34] has been found. For the first time ever it is found that near the RCE surface the unsteady diffusion layer is formed by the reasons of electrolyte turbulent flow.

A new mathematical model of electrochemical codeposition of nanocomposite coatings on the rotating cylindrical electrode, which is taking into account the turbulent flow of the electrolyte, is developed.

The results of hydrodynamic mathematical modeling of copper and alumina particles ECD on RCE with consideration of electrolyte turbulent flow are presented. A good correlation with the published experimental date have been found.

A for first time ever it is found that when the current density achieve their limit value the nonstationary diffusion layer with the variable thickness is formed near the electrode surface by the reasons of electrolyte turbulent flow.

The composition of the MMEC is inhomogeneous both on the length and on the thickness of the composite.

In the future, the authors plan to perform the mathematical modeling of the ECD process using the methods of molecular dynamics, to expand the understanding of the process mechanism.

References

[1] J. L. Stojak, J. Fransaer and J. B. Talbot, "Review of Electrocodeposition," in *Advances in Electrochemical Science and Engineering*, vol. 7, R.C. Alkire, D.M. Kolb, Ed. Weinheim: Wiley-VCH Verlag, 2002, pp. 193-225.

[2] A.Hovestad, L. J. Janssen, "Electroplating of metal matrix composites by codeposition of suspended particles," in *Modern Aspects Of Electrochemistry No. 38*, B. E. Conway, Ed. New York: Kluwer Academic Publishers, 2005, pp.475-532.

[3] A. Gomes, I. Pereira, B. Fernández and R. Pereir, "Electrodeposition of metal matrix nanocomposites: improvement of the chemical characterization techniques," in *Advances in Nanocomposites - Synthesis, Characterization and Industrial Applications*, R. Boreddy, Ed. Rijeka: InTech, 2011, pp.503-526.

[4] J. Bockris, A. Reddy, *Modern Electrochemistry. V. 2, A Fundamentals of Electrodics*, New York: Kluwer Academic Publishers, 2002.

[5] C. G. Fink, J. D. Prince, "The codeposition of copper and graphite," *Transactions of the American Electrochemical Society*, vol. 54, pp. 34-39, Jan. 1928.

[6] R. V. Williams, "Electrodeposited composite coatings," *Electroplating And Metal Finishing*, vol.19, pp. 92-96, Mar. 1966.

[7] L.L. Shaw, "Processing nanostructured materials: an overview," . *Journal of The Minerals, Metals & Materials Society*, vol. 52, pp. 41-45, Dec. 2000.

[8] A. Jung, H. Natter and R. Hempelmann, "Nanocrystalline alumina dispersed in nanocrystalline nickel: enhanced mechanical properties," *The* Journal *of Materials* Science, vol. 44, pp. 2725-2735, Apr. 2009.

[9] F. Hou, W. Wang, H. Guo, "Effect of the dispersibility of ZrO_2 nanoparticles in Ni-ZrO_2 electroplated nanocomposite coatings on the mechanical properties of nanocomposite coatings," *Applied* Surface *Science*, vol.252, pp. 3812-3817, Mar. 2006.

[10] J. Fustes, A. Gomes and M. Silva Pereira, "Electrodeposition of Zn–TiO2 nanocomposite films—effect of bath composition," *Journal of Solid State Electrochemistry*, vol.12, pp. 1435-1443, Jan. 2008.

[11] X. Bin-shi, W. Hai-dou, D. Shi-yun, J. Bin and T. Wei-yi, "Electrodepositing nickel silica nano-composites coatings" *Electrochemistry Communications* vol.7, pp. 572-575, Jun. 2005.

[12] M. Srivastava, J. N. Balaraju, B. Ravishankar, K.S. Rajam, "Improvement in the properties of nickel by nano-Cr2O3 incorporation," *Surface and Coatings Technology*, vol. 205, pp. 66-75, Sep. 2010.

[13] Y. Cho, G. Choi and D. Kim, "A method to fabricate field emission tip arrays by electrocodeposition of single-wall carbon nanotubes and nickel," *Electrochemical and Solid State Letters*, vol. 9, pp. 107-110, Jan. 2006

[14] M. Kaisheva, J. Fransaer, "Influence of the surface properties of SiC particles on their codeposition with nickel," *Journal of The Electrochemical Society*, vol.151, pp.89-96, Jan. 2004.

[15] M. Stroumbouli, P. Gyftou and E. Pavlatou, "Codeposition of ultrafine WC particles in Ni matrix composite electrocoatings," *Surface and Coatings Technology*, vol. 195, pp. 325-332, May 2005.

[16] G.N. Ramesh Bapu, "Electrocodeposition and characterization of nickel-titanium carbide composites," *Surface & Coatings Technology*, vol. 67, pp. 105-110, Sep. 1994.

[17] K. Krishnaveni, S. Narayanan, "Electrodeposited Ni–B–Si3N4 composite coating: Preparation and evaluation of its characteristic properties," *Journal of Alloys and Compounds*, vol. 466, pp. 412-420, Oct. 2008.

[18] A. Hovestad, R. J. Heesen, L.J. Janssen, "Electrochemical deposition of zinc–polystyrene composites in the presence of surfactants," *Journal of Applied Electrochemistry*, vol. 29, pp. 331-338, Mar. 1999

[19] S. Mohan, G. Ramesh Bapu, "Electro-deposition of Nickel-PTFE Polymer composites," *Plating and Surface Finishing*, vol.82, pp.86-88, 1995.

[20] P.C. Tulio, I.A. Carlos, "Effect of SiC and Al2O3 particles on the electrodeposition of Zn, Co and ZnCo: II. Electrodeposition in the presence of SiC and Al2O3 and production of ZnCo–SiC coatings," *Journal of Applied Electrochemistry*, vol.39, pp. 1305-1311, 2009.

[21] M. Ghouse, M. Viswanathan and E.G. Ramachandran, "Electrocodeposition of Nickel Molybdenum Disulfide and Nickel-Tungsten Disulfide," *Metal Finishing*, vol. 78, pp. 44-47, Dec. 1980.

[22] T. Osaka, M. Takai, K. Hayashi, K. Ohashi, M. Satto and K. Yamada, "A soft magnetic CoNiFe film with high saturation magnetic flux density and low coercivity," *Nature*, vol. 392, pp. 796-801, Feb. 1998.

[23] B. Y. Yoo, S.C. Hernandez, D.-Y. Park and N.V. Myung, "Electrodeposition of FeCoNi Thin Films for Magnetic MEMS devices," *Electrochimica Acta*, vol. 51, pp. 6346-6352, Jun. 2006.

[24] E. Gomez, S. Pane and E. Valles, "Magnetic composites CoNi–barium ferrite prepared by electrodeposition" *Electrochemistry Communications*, vol. 7, pp. 1225-1231, Dec. 2005

[25] Y. Sofer, Y. Yarnitzky, S.F. Dirnfeld, "Evaluation and Uses of Composite Ni-Co Matrix Coatings with Diamonds on Steel Applied by Electrodeposition," *Surface and Coatings Technology*, vol.42, pp. 227-236, 1990.

[26] G.A. Malone, "Electrodeposition of Dispersion-Strengthened Alloys," *Plating and Surface Finishing*, vol.78, pp. 58-62, 1991.

[27] R. Mevrel, "State of the Art on High-Temperature Corrosion-Resistant Coatings," *Materials Science and Engineering*, vol.120-121, pp. 13-24, 1989.

[28] S. Pushpavanam, M. Pushpavanam, S. Natarajan, K. C. Narasimham, S. Chinnasamy, "High Surface Area Nickel Cathodes from Electrocomposites," *International Journal of Hydrogen Energy*, vol.18, pp. 277-281, 1993.

[29] M. Lekka, D. Koumoulis, N. Kouloumbi, P.L. Bonora, "Mechanical and Anticorrosive Properties of Copper Matrix Micro- and Nano-Composite Coatings," *Electrochemical Acta*, vol.54, pp. 2540–2546, 2009.

[30] S.-C. Wang, W. Wei, "Kinetics of electroplating process of nano-sized ceramic particle/Ni composite," *Materials Chemistry and Physics*, vol.78, pp. 574-580, 2003.

[31] G. Vidrich, J.-F. Castagnet, H. Ferkel, "Dispersion Behaviour of Al2O3 and SiO2 Nanoparticles in Nickel Sulfamate Plating Baths of Different Compositions," *Journal of The Electrochemical Society*, vol.152, pp. 294-298, 2005.

[32] G. Maurin, A. Lavanant, "Electrodeposition of nickel/silicon carbide composite coatings on a rotating disc electrode," *Journal of Applied Electrochemistry*, vol.25, pp. 1113-1121, 1995.

[33] J.L. Stojak, J.B. Talbot, "Investigation of Electrocodeposition Using a Rotating Cylinder Electrode," *Journal of the Electrochemical Society*, vol.146, pp. 4504-4513, 1999.

[34] J.L. Stojak, J.B. Talbot, "Effect of Particles on Polarization During Electrocodeposition Using a Rotating Cylinder Electrode," *Journal of Applied Electrochemistry*, vol.31, pp. 559-564, 2001.

[35] D. Thiemig, A. Bund, J.B. Talbot, "Influence of Hydrodynamics and Pulse Plating Parameters on the Electrocodeposition of Nickel–Alumina Nanocomposite Films," *Electrochimica Acta*, vol. 54, pp. 2491-2498, 2009

[36] T. Perez, J. Nav, "Numerical simulation of the primary, secondary and tertiary current distributions on the cathode of a rotating cylinder electrode cell. Influence of using plates and a concentric cylinder as counter electrodes," *Journal of Electroanalytical Chemistry*, vol.719, pp. 106–112, 2014.

[37] P. Atempa-Rosiles, et al., "Simulation of turbulent flow of a rotating cylinder electrode and evaluation of its effect on the surface of steel API 5L X-56 during the rate of corrosion in brine added with kerosene and H_2S," *Journal of Electrochemical Science*, vol.9, pp. 4805–4815, 2014.

[38] D.R. Gabe, F.C. Walsh, "The Rotating Cylinder Electrode: a Review of Development," *Journal of Applied Electrochemistry*, vol.13, pp. 3-22, 1983.

[39] D.C. Wilcox, *Turbulence Modeling for CFD*, DCW Industries, 1998.

[40] D.M. Driver, H.L. Seegmiller, "Features of a Reattaching Turbulent Shear Layer in Diverging Channel Flow," *The American Institute of Aeronautics and Astronautics Journal*, vol.23, pp. 163-171, 1985.

[41] K. Abe, T. Kondoh, Y.A. Nagano, "New Turbulence Model for Predicting Fluid Flow and Heat Transfer in Sepa-rating and Reattaching Flows-I. Flow Field Calculations," *International Journal* of Heat and Mass Transfer, vol.37, pp.139-151, 1994.

[42] K.C. Chang, , W.D. Hsieh, C.S. Chen, "A Modified Low-Reynolds-Number Turbulence Model Applicable to Recirculating Flow in Pipe Expansion," *Journal of Fluid Engineering*, vol.117, pp. 417-423, 1995.

[43] B. Launder, B. Sharma, "Application of the Energy Dissipation Model of Turbulence to the Calculation of Flow Near a Spinning Disc," *Letters in Heat and Mass Transfer*, vol.1, pp. 131-138, 1974.

[44] Z. Yang, T.H. Shih, "New Time Scale Based k-ε Model for Near-Wall Turbulence," *The American Institute of Aeronautics and Astronautics Journal*, vol.31, pp. 1191-1198, 1993.

[45] P. Jagadeesh, K. Murali, "Application of Low-Re Turbulence Models for Flow Simulations Past Underwater Vehicle Hull Forms," *Journal of Naval Architecture and Marine Engineering*, vol.1, pp. 41-54, 2005.

[46] E. Fares, , W. Schröder, "A Differential Equation for Approximate Wall Distance," *International Journal for Numerical Methods in Fluids*, vol.39, pp. 743–762, 2002.

[47] A.F. Averill, H.S. Mahmood, "Determination of tertiary current distribution in electrodeposition cell – Part 1 Computational techniques," *Transactions of The Institute of Metal Finishing*, vol.75, pp. 228-233, 1997.

[48] O.C. Zienkiewicz, R.L.Taylor, J.Z. Zhu, *The Finite Element Method: Its Basis and Fundamentals*, Butterworth-Heinemann, 2005.

[49] C.D. Andereck, S.S. Liu, H.L. Swinney, "Flow regimes in a circular Couette system with independently rotating cylinders," *Journal of Fluid Mechanics*, vol.164, pp. 155-183, 1986.

[50] G.I. Taylor, "Stability of a viscous liquid contained between two rotating cylinders," *The Philosophical Transactions of the Royal Society*, vol.223, pp. 289-343, 1923.

[51] A.V. Vakhrushev, E.K. Molchanov, "Hydrodynamic Modeling of Electrocodeposition on a Rotating Cylinder Electrode," *Key Engineering Materials*, vol.654, pp. 29-33, 2015.

[52] M. Eisenberg, C.B. Tobias, C.R. Wilke, "Ionic Mass Transfer and Concentration Polarization at Rotating Electrodes," *Journal of the Electrochemical Society*, vol.101, pp. 306-319, 1954.

[53] C.C. Lee, C.C. Wan, "A Study of the Composite Electrodeposition of Copper with Alumina Powder," *Journal of Electrochemical Society*, vol.135, pp. 1930-1933, 1988.